Investigations of radiation pressure : optical side-band cooling of a trampoline resonator and the effect of superconductivity on the Casimir force

Eerkens, H.J.

7

Simultaneous Calibration Scheme for Casimir Force Measurements

In 1948 Casimir predicted the attractive force between two perfectly conducting plates in a vacuum. But experimental confirmation of this force proved to be difficult due to several factors. The challenge of positioning the two plates perfectly parallel [44, 135] is often circumvented by measuring the force between a plate and a sphere. But two other challenges remain, namely the calibration of the set-up and sphere-plate separation and the presence of the electrostatic force caused by a difference in surface potential between the two materials.

Calibration of the set-up and the distance is often done prior to the Casimir force measurements. Compensation of the electrostatic force is achieved at the start of a measurement run by setting a voltage over the sphere and plate such that the detected force is minimized. The disadvantage of these methods is that it is still sensitive to time-related drifts and distance-dependent contributions to the electrostatic force. That is why we use a method that runs simultaneously with our measurement run [144, 160]. We modulate the electrostatic force at a certain frequency by applying an AC voltage between the sphere and the plate. Based on the modulated force signal we can create a feedback loop that sets the distance at a desired value by adjusting the amplitude of the AC voltage.

In this chapter we will describe this measurement method. We show Casimir force measurements between a gold coated microsphere with radius $R = 100\,\mu$m and a gold coated sapphire plate. We compare our results with calculations of the Casimir force between two gold surfaces to show that our set-up can reliable measure the Casimir force.

7.1 Detection of the plate motion

The set-up is designed to measure forces at submicron distances in a sphere-plate geometry. The gold-coated sphere is attached to an atomic force microscope cantilever that acts as a force sensor. Read-out of the cantilever motion is done using a fiber-optic interferometer. The technique behind fiber interferometry, as well as our sample characterization is described in chapter 6. The cantilever is placed above a gold coated sapphire plate. The measurements were done at room temperature at a background pressure of 2.2×10^{-1} mbar and the whole set-up was placed on an isolated foundation separating it from vibrations from the outside world. A schematic image of the main components of our set-up is shown in Figure 7.1.

The plate is coated with a 150 nm thick layer of gold. It is mounted on a mechanical translation stage consisting of a stick-slip stepper motor (Attocube ANPz101) for coarse approach and a piezo-electric transducer for accurately varying the distance d between the sphere and plate. In this section we will describe the detection of the motion of the plate. In a later section we will show how the electrostatic force is used to relate this motion to the actual sphere-plate distance and to calibrate our force sensitivity.

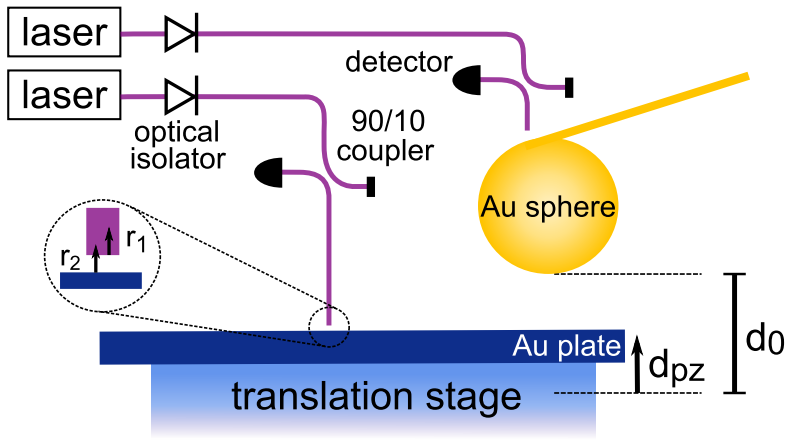

Figure 7.1: Schematic image of the set-up. During a measurement run, the distance d is varied by setting d_{pz} by a translation stage under the gold plate. A force between the gold sphere and plate results in a change in cantilever motion. The motion of both the cantilever and the plate is read out with fiber-optic interferometers. The interferometric signal depends on the interference of light reflected at the fiber end facet (r_1) and at the plate surface (r_2).

During a measurement run, the plate moves towards the sphere in steps. The distance between the sphere and the plate changes with d_{pz} compared to the initial separation d_0, such that the actual sphere-plate distance is equal to $d = d_0 - d_{\mathrm{pz}}$. The distance change d_{pz}, or plate motion, is recorded with a fiber-based common path interferometer [92]. The interferometer is fed by a tunable continuous wave dis-

tributed feedback (CW DFB) laser module (Thorlabs LS5-C-24A-20-NM) operating around $\lambda = 1550\,\mathrm{nm}$. The light is transported via a 90/10 fiber coupler to a cleaved fiber end positioned above the plate. Light reflected at the fiber end (r_1) interferes with light reflected from the plate (r_2) when it passes through the fiber coupler again and falls onto a detector. The interference signal at the detector is given by

$$W_{\mathrm{DC}} = W_0 - W_0 V \cos\left(\frac{4\pi d_{\mathrm{pz}}}{\lambda}\right) \tag{7.1}$$

where W_0 is the midpoint interference signal and V the interferometric visibility. The interferometer is most sensitive for values of d_{pz} where the phases from both reflections are in quadrature. This requirement can only be met for small changes in the distance ($d_{\mathrm{pz}} \ll \lambda/4\pi$). This is not feasible for a typical measurement run, where we want to measure over a distance of several hundred nanometers.

To overcome this issue, the plate motion d_{pz} is modulated at $\omega/2\pi = 119\,\mathrm{Hz}$, with amplitude Δd of roughly $0.5\,\mathrm{nm}$. Following a Taylor expansion, the interference signal now also contains an oscillating component in phase quadrature with the original signal, with amplitude

$$W_\omega = \frac{4\pi W_0 V \Delta d}{\lambda} \sin\left(\frac{4\pi d_{\mathrm{pz}}}{\lambda}\right). \tag{7.2}$$

A point with low sensitivity in one term is now compensated by a high sensitivity in the other term. The distance change d_{pz} can be deduced from the phase-angle between the two terms:

$$d_{\mathrm{pz}} = \frac{\lambda}{4\pi} \arctan\left(\frac{\lambda}{4\pi\Delta d}\frac{W_\omega}{W_0 - W_{\mathrm{DC}}}\right). \tag{7.3}$$

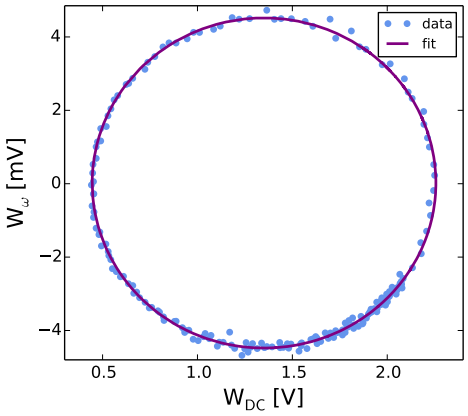

Figure 7.2: Lissajous plot of the two components of the plate interferometer signal, W_ω and W_{DC} (blue dots). The resulting ellipse is fitted (purple line) to find the distance change d_{pz}.

During a measurement run, the DC level of the detector signal from the plate interferometer, W_{DC}, is low-pass filtered and recorded with an ADC and the modulated signal W_ω with a lock-in amplifier with time constant 30 ms. To determine the values for W_0 and Δd, it is possible to fit W_{DC} and W_ω separately. But a more convenient choice is to display the two signals in a Lissajous plot and fit the resulting ellipse. Both the data and the fit are shown in Figure 7.2.

The correspondence between the fit and data tells us that the plate interferometer is well able to follow the plate motion and that disturbing effects such as external vibrations or piezo creep do not affect our measurements. From the axes and the center position we can deduce $W_0 = 1.35\,\mathrm{V}$, $\Delta d = 0.61\,\mathrm{nm}$ and the plate interferometric visibility $V = 0.67$. Using these values and Eq. 7.3 we can then determine d_{pz}. To calibrate the offset distance d_0 and therefore the actual distance between the sphere and the plate, we use the electrostatic force. In the next section we will explain the calibration method.

7.2 Calibration with the electrostatic force

The force sensor is based on a doped silicon micromechanical cantilever with nominal spring constant $k = 0.9\,\mathrm{N/m}$ (Bruker RESP-20). A polystyrene sphere (Thermo Scientific 4320A) with radius $R = 100\,\mu\mathrm{m}$ is attached at the end of it. Both the sphere and the cantilever are covered with a 200 nm conductive gold coating. The cantilever motion and resonance frequency ($f_0 = 2.3\,\mathrm{kHz}$) are read out by a second fiber-optic interferometer, positioned $200\,\mu\mathrm{m}$ from the cantilever and fed by a second, similar laser source. The laser frequency is tuned to quadrature point corresponding to the fiber-cantilever distance. A self oscillating circuit [161] drives the cantilever at its resonance frequency to ensure a constant cantilever amplitude of roughly 1 nm RMS.

With this force sensor we wish to detect the Casimir force F_C, but there also exists an electrostatic force caused by a voltage across the plate and the sphere. Even when there is no external voltage applied, there exists a contact potential difference V_0 caused by a difference in the materials' work functions. This difference can also exist between two surfaces of the same material, since different application circumstances may lead to variations in crystal face or in possible contamination. Although the electrostatic force can easily overcome the Casimir force in magnitude, it allows us to calibrate our force sensor and the actual distance between the sphere and plate as well as to detect and compensate V_0.

Because the electrostatic force depends on the potential difference between the sphere and the plate, it can be altered we apply an additional voltage. More specifically, since the Casimir force does not depend on the voltage across the sphere and the plate, modulating this voltage at a known frequency allows us to separate the two forces. The signal from the force sensor at the modulation frequency $\omega_1/2\pi = 72.2\,\mathrm{Hz}$ only shows the electrostatic contribution. The total voltage across the sphere and plate consists of an applied AC and DC voltage, plus the naturally present contact potential difference V_0:

$$V = V_0 + V_{\mathrm{DC}} + V_{\mathrm{AC}} \cos(\omega_1 t). \tag{7.4}$$

We use the expression $F_{\rm ES} = -\pi\varepsilon_0 R V^2/d$ for the electrostatic force in a sphere-plate geometry, with ε_0 the vacuum permittivity. This expression is an approximation that holds in the limit of small distance compared to the sphere radius [138]. Later in this section we will check its validity. The total electrostatic force acting on the cantilever has multiple frequency components as well as a static component:

$$F_{\rm ES} = -\frac{\varepsilon_0 \pi R}{d}\left[(V_0+V_{\rm DC})^2 + 2(V_0+V_{\rm DC})V_{\rm AC}\cos(\omega_1 t) + \frac{1}{2}V_{\rm AC}^2 + \frac{1}{2}V_{\rm AC}^2\cos(2\omega_1 t)\right]. \tag{7.5}$$

The total force between the sphere and plate is detected as a change in the cantilever motion, where the cantilever's static deflection, oscillation amplitude and resonance frequency are influenced. The cantilever is deflected in accordance to Hooke's law, which results in a interferometer signal S given by

$$S = \frac{\gamma(F_C + F_{\rm ES})}{k}, \tag{7.6}$$

with γ the sensitivity of the interferometric read-out in units of V/m. When the force oscillates slowly compared to the cantilever's resonance frequency, the cantilever can easily move in phase with the force. We will call this method of detection the quasi-static (QS) detection.

Since the electrostatic force has different frequency components, the signal can also be divided into different parts:

$$S = S_{\rm s} + S_{\omega_1}\cos(\omega_1 t) + S_{2\omega_1}\cos(2\omega_1 t), \tag{7.7}$$

with static deviation and oscillation amplitudes given by

$$S_{\rm s} = \frac{\gamma F_{\rm C}}{k} - \frac{\gamma\pi\varepsilon_0 R}{kd}(V_0+V_{\rm DC})^2 - \frac{\gamma\pi\varepsilon_0 R}{2kd}V_{\rm AC}^2 \tag{7.8}$$

$$S_{\omega_1} = -\frac{2\gamma\pi\varepsilon_0 R}{kd}(V_0+V_{\rm DC})V_{\rm AC} \tag{7.9}$$

$$S_{2\omega_1} = -\frac{\gamma\pi\varepsilon_0 R}{2kd}V_{\rm AC}^2 = -\frac{\kappa}{2d}V_{\rm AC}^2, \tag{7.10}$$

with $\kappa = \gamma\pi\varepsilon_0 R/k$ the force sensitivity. The amplitudes are detected with lock-in amplifiers (time constant 300 ms) set directly on the cantilever interferometer signal. The static deviation can be influenced by drifts, which makes it an unreliable measure for the Casimir force. It is possible to modulate the Casimir force as well [160] by slightly oscillating the plate, thereby modulating the distance. But since our cantilever interferometer is very sensitive to spurious reflections from the plate (see chapter 6), we cannot separate the modulated Casimir force from the modulated plate motion. That is why we use a different detection method.

Since the force between the sphere and plate depends on separation, there exists a force gradient that changes the cantilever's resonance frequency according to [161]

$$\Delta f = -\frac{f_0}{2k}\frac{\partial(F_C + F_{\rm ES})}{\partial d}. \tag{7.11}$$

A static force gradient leads to a frequency shift, while an oscillating force gradient results in a frequency modulation. We will refer to this force gradient detection method as the frequency modulation (FM) detection. There are also different components in the cantilever frequency change

$$\Delta f = \Delta f_{\mathrm{s}} + \Delta f_{\omega_1}\cos(\omega_1 t) + \Delta f_{2\omega_1}\cos(2\omega_1 t). \tag{7.12}$$

with static frequency shift and frequency deviations given by

$$\Delta f_{\mathrm{s}} = f - f_0 = -\frac{f_0}{2k}\frac{\partial F_{\mathrm{C}}}{\partial d} - \frac{f_0\pi\varepsilon_0 R}{2kd^2}(V_0 + V_{\mathrm{DC}})^2 - \frac{f_0\pi\varepsilon_0 R}{4kd^2}V_{\mathrm{AC}}^2 \tag{7.13}$$

$$\Delta f_{\omega_1} = -\frac{f_0\pi\varepsilon_0 R}{kd^2}(V_0 + V_{\mathrm{DC}})V_{\mathrm{AC}} \tag{7.14}$$

$$\Delta f_{2\omega_1} = -\frac{f_0\pi\varepsilon_0 R}{4kd^2}V_{\mathrm{AC}}^2 = -\frac{\mu}{2d^2}V_{\mathrm{AC}}^2, \tag{7.15}$$

where we assign the system parameter $\mu = f_0\pi\varepsilon_0 R/2k$. Since a lock-in amplifier doesn't detect frequencies, we send the cantilever interferometer signal through a frequency-to-voltage converter that detects the cantilever frequency and translates it linearly to a DC voltage. Frequency modulations translate to modulations of the voltage, with the frequency deviation equal to the amplitude of the signal at the modulation frequency. The static frequency shift can be used to extract the Casimir force gradient. We detect the instantaneous cantilever frequency using a home-built software radio and a frequency counter (Agilent 53131A) on the (filtered) cantilever interferometer signal. We also use the phase-locked loop option of our lock-in amplifier (Zurich Instruments HF2LI). To obtain the frequency shift, we determine f_0 from data points far away enough that the Casimir force has an undetectable influence. The instantaneous frequency there is only affected by the known electrostatic force, which we can subtract to obtain f_0.

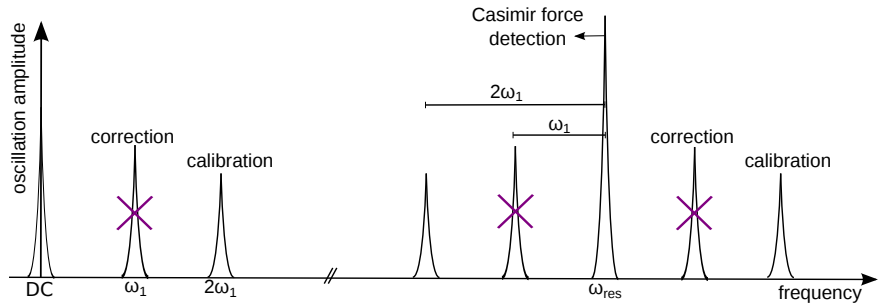

Figure 7.3: Frequency components in the cantilever interferometer signal. The quasi-static signals are at the low-frequency range of the spectrum, at ω_1 and $2\omega_1$. The frequency modulation signals appear as double side-bands around the resonator frequency. The signals at ω_1 are used to correct for the contact potential difference, via a feedback loop that minimizes these signals by applying a compensating DC voltage. The signals at $2\omega_1$ are used to calibrate the system. The Casimir force is detected as a shift in the cantilever resonance frequency.

An overview of the frequency components of our cantilever interferometer signal is shown in Figure 7.3. The quasi-static signals are located near DC and the frequency modulation signals appear as double sidebands around the resonance frequency of the cantilever. Both QS and FM signals can be used to calibrate the system and correct for the contact potential difference. The static shift of the resonance frequency is used to measure the Casimir force gradient.

We will first discuss how the influence of the contact potential difference is compensated using a technique similar to what is used in Kelvin probe force microscopy [162]. Note that the QS amplitude S_{ω_1} as well as the frequency deviation Δf_{ω_1} are proportional to the sum of the contact potential difference and our applied DC voltage. Both terms are linear in V_{DC} and are zero when $V_{\mathrm{DC}} = -V_0$, i.e. when the contact potential difference is compensated. We have checked that this is true by sweeping the DC voltage while measuring S_{ω_1} and Δf_{ω_1}. Both lines should be linear and cross zero at the same point. The result is shown in Figure 7.4. These data were obtained at room temperature between the gold sphere and plate separated by roughly $1\,\mu$m. During the sweep we applied an AC voltage of $1\,\mathrm{V_{pp}}$. The results are indeed linear in V_{DC} and both signals are zero around the same DC voltage, although a slight offset exists. The FM signal decreases faster with distance than the QS signal. At the relative large distance of $1\,\mu$m, it is therefore not surprising that it is more influenced by noise. Note that even between two gold surfaces at room temperature, we detect a contact potential difference of $61\,\mathrm{mV}$. This is probably caused by different circumstances in the coating process and/or the different substrates.

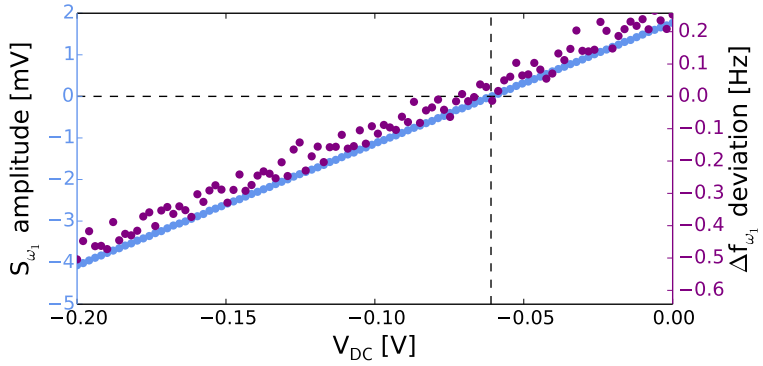

Figure 7.4: The QS and FM signals at ω_1 as a function of the DC voltage; S_{ω_1} (blue) and Δf_{ω_1} (purple). Both signals are linear in V_{DC} and cross zero at the same DC voltage, indicating a contact potential difference of $61\,\mathrm{mV}$ between two gold surfaces.

Knowing V_0, we can simply set V_{DC} at the start of a measurement. But since V_0 can change over time during a measurement, we create a feedback loop keeping either S_{ω_1} or Δf_{ω_1} zero. In Figure 7.5 we show the output DC voltage from the feedback loop during a measurement run, as well as the remaining potential difference calculated from S_{ω_1}.

The contact potential difference is fed back up to only a few millivolts during the

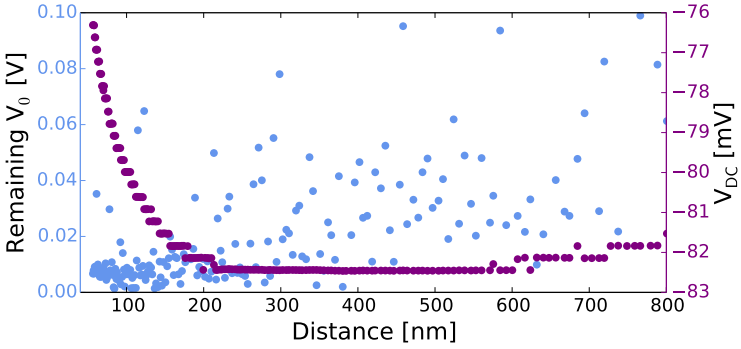

Figure 7.5: Result of the electrostatic compensation scheme. From the quasi-static signal S_{ω_1} can be calculated that the surface potential V_0 is successfully reduced. The remaining potential as a function of distance is shown in blue. The output DC voltage (purple), equal to $-V_0$, changes as a function of distance.

whole measurement run. However, there is a clear distance-dependence of the output DC voltage. This would suggest that the mean surface potential V_0 is distance-dependent, but it is only determined by the material properties. There are several possible explanations for the behaviour in our measurements. One is the presence of another conductor, for example the cantilever or the sample mount, that is gradually shielded during approach [163]. Another explanation is the influence of variations in the surface potential, which leads to an electrostatic force with a different distance-dependence than following from the mean surface potential [164, 165]. The presence of this extra force shows that compensating for V_0 only at a far away distance is not sufficient and that a real-time compensation scheme is clearly needed.

Apart from compensation, the electrostatic force is used to calibrate the force sensitivity of the set-up and the distance between the sphere and the plate. As described in the previous section, we use a fiber interferometer positioned above the plate to determine the distance the plate moves during one measurement run, d_{pz}. The sphere-plate distance is equal to $d = d_0 - d_{\mathrm{pz}}$. The initial separation d_0 is obtained from a fit to the electrostatic signals at $2\omega_1$. Instead of fitting $S_{2\omega_1}$ directly, we rewrite Eq. 7.10 as $V_{\mathrm{AC}}^2/(2S_{2\omega_1}) = (d_0 - d_{\mathrm{pz}})/\kappa$, which is linearly dependent on d_{pz}. Similarly, we can rewrite Eq. 7.15 as $V_{\mathrm{AC}}/\sqrt{2\Delta f_{2\omega_1}} = (d_0 - d_{\mathrm{pz}})/\sqrt{\mu}$. The data from a typical measurement run based on the QS signals is shown in Figure 7.6(a), and based on the FM signals in Figure 7.6(b). The fits follow the data, especially at large d_{pz} where the distance between the sphere and the plate is smallest and the electrostatic force is largest. From the fit we can determine an offset distance $d_0 = 832\,\mathrm{nm}$ which we can use to deduce the actual sphere-plate distance.

From the slope of the fit in Figure 7.6(a) we can determine the force sensitivity $\kappa = 1.69 \times 10^{-8}\,\mathrm{m\,V^{-1}}$. This value is close to the expected value of $\kappa = 2 \times 10^{-8}\,\mathrm{m\,V^{-1}}$ based on the values $k = 0.9\,\mathrm{N/m}$, $R = 100\,\mu\mathrm{m}$ and $\gamma = 7\,\mathrm{MV/m}$. The difference is caused in uncertainties in the spring constant and/or sphere radius. The interferometric sensitivity γ can be determined separately from the cantilever interferometer

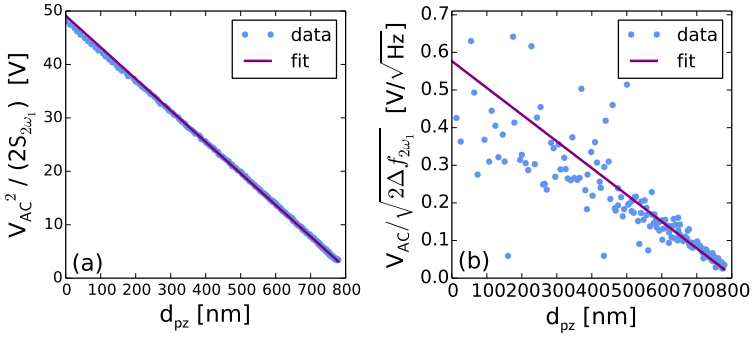

Figure 7.6: Data (blue dots) and fit (purple line) used to find the offset distance d_0 from the modulated electrostatic force: (a) $V_{\mathrm{AC}}^2/(2S_{2\omega_1})$ as a function of the distance change d_{pz}; (b) $V_{\mathrm{AC}}/\sqrt{2\Delta f_{2\omega_1}}$ as a function of the distance change d_{pz}.

signal as a function of the laser frequency. The system parameter μ is found from the fit in Figure 7.6(b), $\mu = 1.98 \times 10^{-12}\,\mathrm{Hz\,m^2\,V^{-2}}$, close to the calculated value of $3.55 \times 10^{-12}\,\mathrm{Hz\,m^2\,V^{-2}}$.

Once we know these parameters, we can determine the distance from the ratio between either $S_{2\omega_1}$ or $\Delta f_{2\omega_1}$ and the AC voltage V_{AC}:

$$d = \frac{\kappa V_{\mathrm{AC}}^2}{2S_{2\omega_1}} = \sqrt{\frac{\mu V_{\mathrm{AC}}^2}{2\Delta f_{2\omega_1}}}. \tag{7.16}$$

This approach is preferable, because it is less sensitive to noise in our plate interferometer. It also allows us to set the distance by applying a certain AC voltage and creating a feedback loop that moves the piezo-electric transducer until the corresponding electrostatic force signal (either $S_{2\omega_1}$ or $\Delta f_{2\omega_1}$) is reached. This way it is possible to reach a certain distance by simply setting the AC bias voltage. We typically do one measurement run with an educated guess for either κ or μ, then we determine the correct values for κ and μ from the fits such that we can set the desired distances for the following runs. It is even possible to do a measurement run where we keep the distance fixed at one value. This allows us to directly measure the effect of the superconducting transition by sweeping the temperature across the critical temperature, without the influence of drift or thermal expansion.

7.2.1 Validity of the proximity force approximation

As mentioned before, our calibration scheme is based on an approximation of the electrostatic force. Here we will check the validity of this approximation by comparing it to the full electrostatic force. From the self-capacitance of the sphere and plate and their mutual capacitance it is possible to find a complete expression [166]:

$$F_{\mathrm{ES}} = 2\pi\varepsilon_0 V^2 \sum_{n=1}^{\infty} \frac{\coth(\alpha) - n\coth(n\alpha)}{\sinh(n\alpha)} \tag{7.17}$$

with $\alpha = \text{arccosh}(1 + d/R)$. We approximated the infinite sum by taking the first 100.000 terms. Within the precision of our calculations, we could see no change when more terms were taken into consideration.

It is possible to calculate the sum at several distances and calibrate our measurement with (an interpolation of) the full electrostatic theory. But this is may be an unnecessarily complex method if a more simple expression is also valid. For practical purposes, we use the expression given in Eq. 7.5. This expression is obtained via the Proximity Force Approximation (PFA) [136–138] that relates the force in a sphere-plate geometry (F_{sp}) to the free energy per unit area in a parallel-plate geometry (U_{pp}):

$$F_{\text{sp}}(d, R) \approx 2\pi R U_{\text{pp}}(d). \tag{7.18}$$

From the energy per unit area of two infinite parallel conducting plates, $U_{\text{pp}}(d) = \varepsilon_0 V^2/2d$, we deduce the expression given in Eq. 7.5. It must be noted, however, that the PFA only holds under two conditions: the interaction energy must be localized and the distance of closest approach must be small compared to the sphere radius ($d \ll R$). In our set-up we have a $100\,\mu$m radius sphere at a distance of less than $1\,\mu$m from the plate. So the condition is only met up to 1%. To see if this indeed leads to errors in our measurements, we look at the QS electrostatic signal $S_{2\omega_1}$ as a function of distance. During a typical measurement run we keep this signal constant in a feedback loop that adjusts the distance to match a given AC voltage. There should therefore be a linear dependence between V_{AC}^2 and the distance as long as the electrostatic approximation holds. In Figure 7.7 we show data obtained during a typical Casimir force measurement run. The black dots show the applied AC voltage as a function of distance. The two lines indicate the calculated AC voltage based on experimental parameters, either using the approximation or the full theory. The purple line is derived from the approximation according to

$$V_{\text{AC,approx}}^2 = \frac{2kdS_{2\omega_1}}{\gamma\varepsilon_0\pi R}. \tag{7.19}$$

The distance here is derived with our calibration method based on the approximated expression for the electrostatic force. The blue line is obtained using the full electrostatic force and is given by

$$V_{\text{AC,full}}^2 = \frac{kS_{2\omega_1}}{\gamma\pi\varepsilon_0}\left(\sum_{n=1}^{100.000}\frac{\coth(\alpha) - n\coth(n\alpha)}{\sinh(n\alpha)}\right)^{-1}. \tag{7.20}$$

In both calculations we have used the measured value of $S_{2\omega_1}$. The ratio k/γ is derived from the calibration of κ, with the value $R = 100\,\mu$m. The sum is calculated for 2000 distances between $d = 100\,$nm and $10\,\mu$m and then interpolated with the distances from our measurement.

From the overlap in Figure 7.7(a) it is clear that both the full electrostatic force and the approximation describe our data well within the measurement fluctuations. This is even better visible in the residuals between the data and the two calculations shown in Figure 7.7(b). The two calculations start to deviate from each other at a distance larger than $700\,$nm, which shows the limits of the PFA. But it is clear that we can safely use the approximated electrostatic force for our calibration scheme.

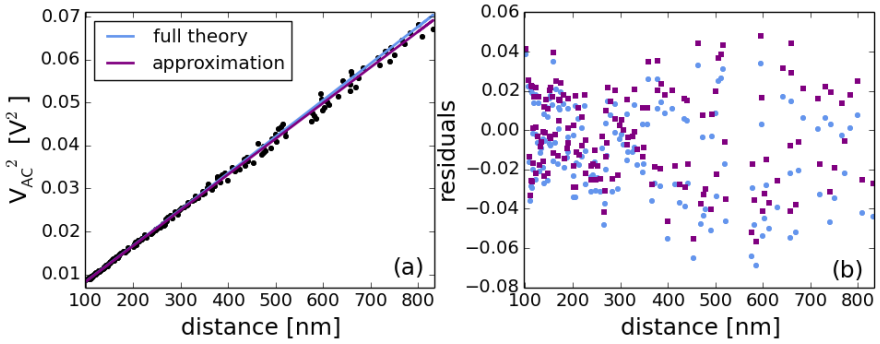

Figure 7.7: Comparison of electrostatic force approximation with full theory: (a) V_{AC}^2 as a function of distance, both measured experimentally (black dots) and calculated from either the full electrostatic force (blue line) or its approximation (purple line). Any deviation from linear dependence shows that the approximation no longer holds; (b) Residuals of the measurements in (a) show negligible deviation compared to the fluctuations in the measurement.

7.3 Casimir force measurements

In the previous section we described how we use the electrostatic force to compensate the contact potential difference and to set the distance at a fixed value. We mentioned that this calibration scheme operates simultaneously with our Casimir force measurements. The Casimir force gradient itself is obtained from the static frequency shift Δf_{s} given by Eq. 7.13. When V_0 is compensated, the middle term on the right hand side in this equation is zero. The other terms can be rewritten to give the Casimir force gradient, normalized to the sphere radius:

$$\frac{1}{R}\frac{\partial F_C}{\partial d} = \frac{\epsilon_0 \pi}{\mu}[\Delta f_{2\omega_1} - \Delta f_{\mathrm{s}}]. \tag{7.21}$$

Via the proximity force approximation we can compare this to theoretical computations of the Casimir force in the parallel-plate geometry, since the measured, normalized, Casimir force gradient only differs a factor 2π from the calculated pressure.

The result of one of our measurement runs between two gold surfaces at room temperature is shown in Figure 7.8. During this run the distance feedback was active, setting the distance at 200 logarithmically distributed values between $800\,\mathrm{nm}$ and $56\,\mathrm{nm}$. The feedback was set on the quasi-static signal $S_{2\omega_1}$, with set-point $0.5\,\mathrm{mV_{rms}}$ and based on a force sensitivity $\kappa = 1.69 \times 10^{-8}\,\mathrm{m\,V^{-1}}$. This set-point corresponds to a force amplitude at $2\omega_1$ of $0.1\,\mathrm{nN}$. A second feedback loop was set to minimize S_{ω_1} by applying a DC voltage of about $80\,\mathrm{mV}$, this value changed with distance.

The calculation shown in the same plot is done according to the Lifshitz theory using the Drude model for the reflectivity of the gold surfaces [112]. For an explanation of these calculations we refer to chapter 5. There may be slight deviations due

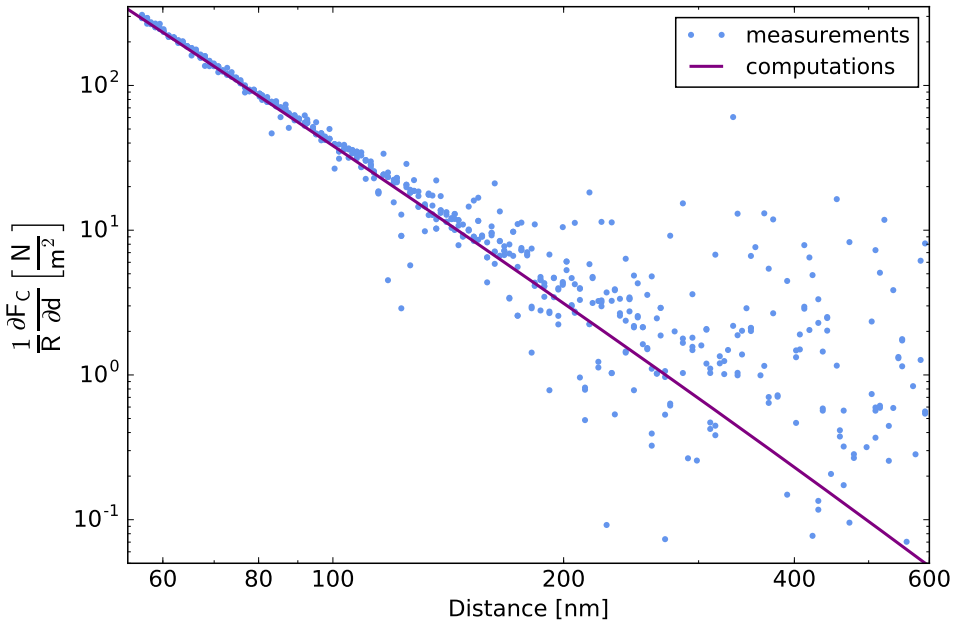

Figure 7.8: Casimir force gradient, normalized to the sphere radius, between a sapphire plate coated with $150\,\text{nm}$ gold and a $100\,\mu\text{m}$ radius sphere with a $200\,\text{nm}$ gold coating. The measurement was performed at room temperature with a background pressure of $2.2 \times 10^{-1}\,\text{mbar}$. The good overlap between calculations and measurements shows that we can reliably measure the Casimir force with a method based on simultaneous calibration with the electrostatic force.

to surface roughness or the specific optical properties of our samples. Also the calculated Casimir force would be somewhat larger if it was based on the plasma model. However, these deviations will be less than a percent compared to the calculations shown in the figure. This is still within the precision of our measurements which is of the order of several percent.

From the good overlap between experiment and theory it is clear that our set-up is capable of detecting the Casimir force gradient between two gold surfaces in a sphere-plate geometry. It is also clear that there persist no systematic errors in our set-up, at least no errors larger than the measurement fluctuations of order $1\,\text{N/m}^2$. This means that with our electrostatic force calibration scheme, we can reliably measure the Casimir force gradient in the range $50 - 200\,\text{nm}$. This scheme also allows us to measure the temperature dependence directly by setting the distance at a certain value and keeping it fixed while we sweep the temperature. The next step is to exchange the gold coated plate for a plate coated with a superconductor.